Islamic Azad University
Mashhad Branch

Moslempour et al. / Iranian Journal of Earth Sciences 9 (2017) / 1-16

Petrogenesis of mantle peridotites from the South of Jazmourian, Makran accretionary prism, Iran

Mohammad Elyas Moslempour*[1], Morteza Khalatbari-Jafari[2], Tomoaki Morishita[3], Habib Biabangard[4]

1. Department of Geology, Research Center for Earth Science, Zahedan Branch, Islamic Azad University, Zahedan, Iran
2. Research Institute for Earth Science, Geological Survey of Iran, Tehran, Iran
3. School of Natural System, College of Science and Engineering, Kanazawa University, Japan
4. Department of Geology, Faculty of Science, University of Sistan and Baluchestan, Zahedan, Iran

Received 11 May 2016; accepted 3 November 2016

Abstract

Mantle peridotites exposed in south Jazmourian comprise of lherzolite and porphyroclastic Cpx-bearing harzburgite in the lower part with chromitite lenses in the upper parts. Petrography and microprobe studies shows evidence of melt-peridotite interactions; post melting processes and subsolidus interactions, which has been associated with appearance of two generations of deformed primary pyroxene-olivine and fine-grained pyroxene-olivine-amphibole neoblasts. Second generation of minerals formed as inclusion, interstitial and fine-grain. These two groups of minerals have different geochemical characteristics, So that, the first group are comparable with abyssal peridotites and second group are comparable to suprasubduction (SSZ) peridotites. Thus, the chemical compositions of different generations minerals show different petrogenesis for ultramafic rocks in south Jazmourian. Whole rock chemical data indicate south Jazmourian peridotites have a depleted MORB mantle source which undergoing 10-20% partial melting. Thus this peridotites have experienced multistage evolution and show characteristics of the abyssal environment to suprasubduction zone. We are belived that peridotites transition from the abyssal environment to suprasubduction and affected by fluids derived from the subducted slab.

Keywords: *Iran, Makran, Jazmourian, Peridotite, Supra-subduction zone (SSZ)*

1. Introduction

Makran accretionary prism is one of the most extensive accretionary complexes in the word (Shahabpour 2010). The accretionay wedge grew seaward by accretion of trench fill sediments, and by slope, shelf and coastal plain progradation (Shahabpour 2010). At present, the accretionary complex has an along-strike extent of about 1000 Km and is separated by two fault systems from regions of active continent– continent collision (the Zagros and Himalaya) (Kopp et al. 2000).

Iranian ophiolites are a part of the Tethyan ophiolite belt of the Middle East. They link the Middle Eastern and Mediterranean and Hellenides–Dinaride ophiolite (e.g. Turkish, Troodos, Greek and East European) to more easterly Asian ophiolites (e.g. Pakistani and Tibetan) (Shojaat et al. 2003) Geographically, the Iranian ophiolites have been divided into four groups (McCall 1997; Stöcklin 1974; Takin 1972): (i) Ophiolites of northern Iran along the Alborz range; (ii) Ophiolites of the Zagros Suture Zone, including the Neyriz and Kermanshah ophiolites, which appear to be coeval with the Samail (Oman) ophiolite emplaced onto the Arabian continental margin; (iii) Unfragmented ophiolites of the Makran accretionary prism, which includes the complex of Fannuj-Maskutan; and (iv) Ophiolites and colored melanges that mark the boundaries of the Central Iranian Microcontinent (CIM), including Shahr-e-Babak, Naien, Baft, Sabzevar and Tchehel Kureh ophiolites (Fig. 1).

Ophiolites in Makran accretionary prism has divided in four groups (McCall 1985; McCall 1997; McCall 2003), Band-e-Zeyarat/Dar Anar, Ganj, Remeshk-Mokhtarabad and Fannuj-Maskutan ophiolitic complex. In later years were studied ophiolites of Band-e-Zeyarat/DarAnar by Ghazi et al. (2004) and Kananian (2000), Ganj by Shaker Ardakani (2009), Remeshk-¬Mokhtarabad by Rastin (1999), Fannuj-Maskutan by Desmons and Beccaluva (1983); Mohajeran (1998); Hunziker et al. (2010); Moslempour et al. (2015); Moslempour et al. (2013) and Iranshahr ophiolites by Omrani et al. (2017). The ophiolites in Makran accretionary prism compared with other Iranian ophiolite, shows a more complete sequence of a classical ophiolite, and while these ophiolites need more studies.

Desmons and Beccaluva (1983) and Mohajeran (1998) based on geochemical studies on extrusive sequence in Maskutan and Sarzeh areas, proposed mid oceanic ridge environment for the formation of Fannuj-Maskutan ophiolite. Desmons and Beccaluva (1983) also, have not ruled out the possibility of a back-arc basin for Fannuj-Maskutan ophiolite. McCall (1985) according to studies

*Corresponding author.
E-mail address (es): memoslempour@yahoo.com

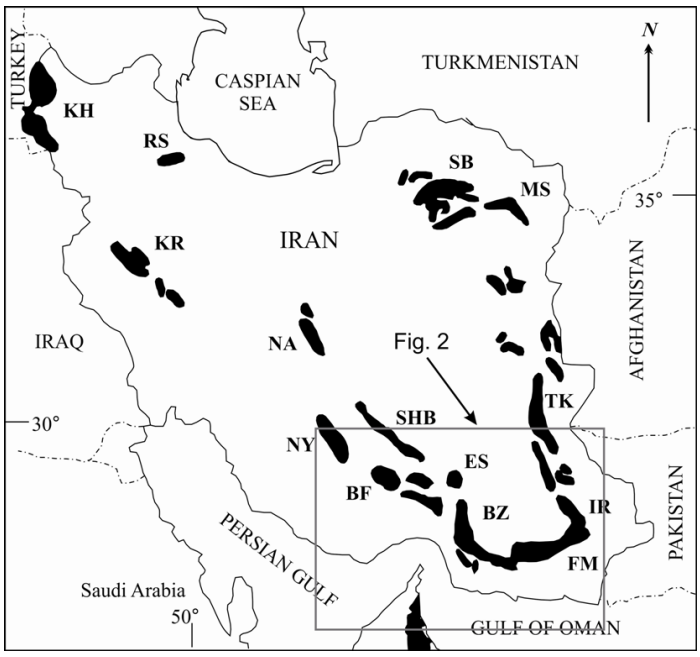

Fig 1. Locations of major Iranian ophiolites. Khoy (KH), Kermanshah (KR), Neyriz (NY), Naien (NA), Shahr-e-Babak (SHB), Baft (BF), Esphandagheh (ES), Band-e-Zeyarat (BZ), Fannuj-Maskutan (FM), Iranshahr (IR), Tchehel Kureh (TK), Mashad (MS), Sabzevar (SB), Rasht (RS).

in the Makran region, proposed a back arc basin environment for the formation of Makran ophiolitic complexes. Kananian (2000) has believed Kahnuj ophiolitic complex to a marginal basin (back-arc) which was located between Bajgan and Lut continental blocks. Hunziker et al. (2010) based on geochemical studies, attributed the blue schists of South Jazmourian, with a subduction zone and Moslempour et al. (2015); Moslempour et al. (2013) proposed an SSZ environment for evolution of Fannuj-Maskutan ophiolite. In this article, we present the first result of gochemical studies on mantle section rocks in the south Jazmourian.

2. Geological background

Iranian Makran continental margin bordered by Oman Sea at the south and a folded and faulted accretionary sediment and colored mélange wedge which extends several hundred kilometers inland toward north (Fig. 2). There are three important geologic features in southeastern Iran: (i) the Makran accretionary prism, which formed as a result of the subduction of Tethyan crust beneath the Eurasian plate or the CIM; (ii) the Jazmourian depression, which is located at the southern end of the Lut Block (north the Makran accretionary prism) and has been considered as a back-arc basin related to the Makran subduction zone (Glennie et al. 1990; Glennie 2000; McCall 1985; McCall 1997; McCall and Kidd 1982); and (iii) a zone of Cenozoic volcanic and plutonic rocks of andesitic to rhyolitic composition which are thought to represent the volcanic arc related to the Makran subduction zone (Farhoudi and Karig 1977).

Mantle section rocks are exposed in the central part of the structural zone of Makran, the south-eastern Iran and southern margin of the Jazmourian depression and represents the remains of Neo-Tethys related branch oceanic crust with Mesozoic age (Desmons and Beccaluva 1983; McCall 1985; McCall 1997; McCall 2002; Sengor et al. 1998). This ophiolitic complex with an area of more than 2800 Km^2 is one of the largest and most complete ophiolitic complexes in Iran (Desmons and Beccaluva 1983; McCall 1985; McCall 1997) which is considered as part of the Alpine-Himalayan ophiolite belt (Desmons and Beccaluva 1983; McCall 1985; McCall 1997). Based on classification of Knipper et al. (1986), the study area is located in Makran-Zahedan ophiolitic group, which has a tectonic boundary from the West with Peri-Arabic ophiolitic belt, that described by Ricou (1977). In this complex, there are many lenticular shaped masses with east-west trends located in south Jazmourian depression. In south Jazmourian, mantle sequence rocks are outcrop in western part and toward to east exposed crustal sequence rocks (Fig. 3).

The south Jazmourian mantle sequence includes lherzolite and porphyroclastic clinopyroxene-bearing harzburgite, fine-grained lherzolite with neocrystals, and scattered lenses of dunite and chromitite. Despite serpentinization, these units display evidence for mantle and asthenosphere textures.

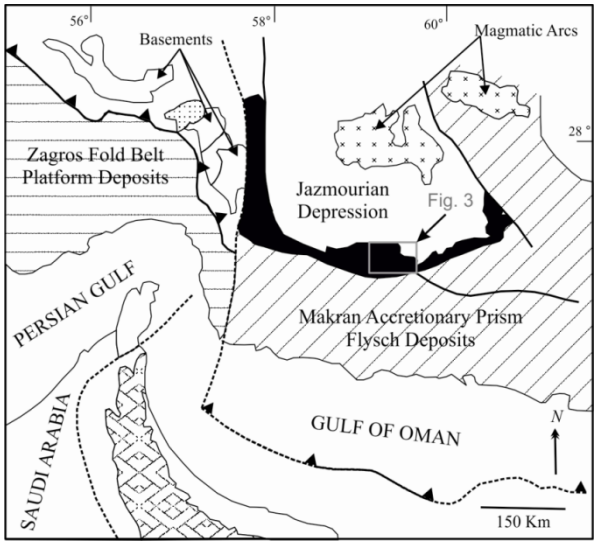

Fig 2. generalised geology map of the Iranian Makran, modified from Gregory et al. (1998).

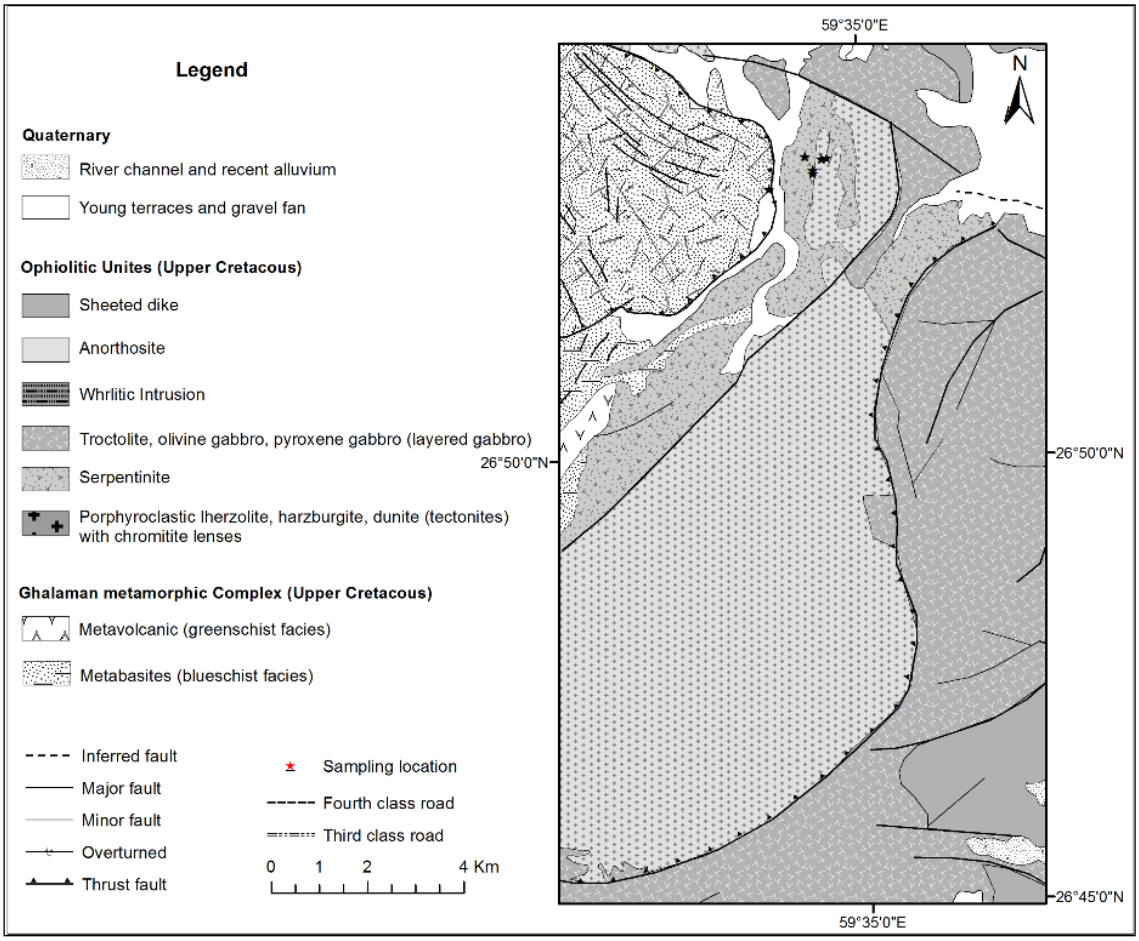

Fig 3. Geological map of studied area (modified from the geological map of Iran, Fannuj sheet; Series 1:100,000)

The peridotite in the south Jazmourian ophiolite can be divided into two groups. The first group lies at the base of the mantle sequence and extends from north of Fannuj to south of the village of Aparang (Fig. 4). This group includes porphyroclastic clinopyroxene-bearing harzburgite and porphyroclastic lherzolite and displays textural evidence for mantle deformation. These include high-temperature, plastic porphyroclastic texture and mantle foliation. The mantle deformation is evidenced by kinked porphyroclastic olivine, stretched porphyritic enstatite, and rotated clinopyroxene porphyroclasts that match those interpreted as evidence for mantle deformation in ophiolites (Juteau and Maury 2012; Nicolas 2012). The peridotite of the second group is exposed as small outcrops to the south, east, and west of the town of Fannuj (Fig. 4), and it displays cumulate textural characteristics with scarce evidence for mantle deformation. The second group of peridotite is cut by isolated gabbroic and diabase dikes and features that are common in asthenospheric peridotite, such as boudinaged pyroxenite sills and dikes with varying thicknesses (Dijkstra et al. 2009; Marchesi 2006; Suhr et al. 2008). Plagioclase, clinopyroxene, and occasionally olivine veins and veinlets also cut the peridotite.

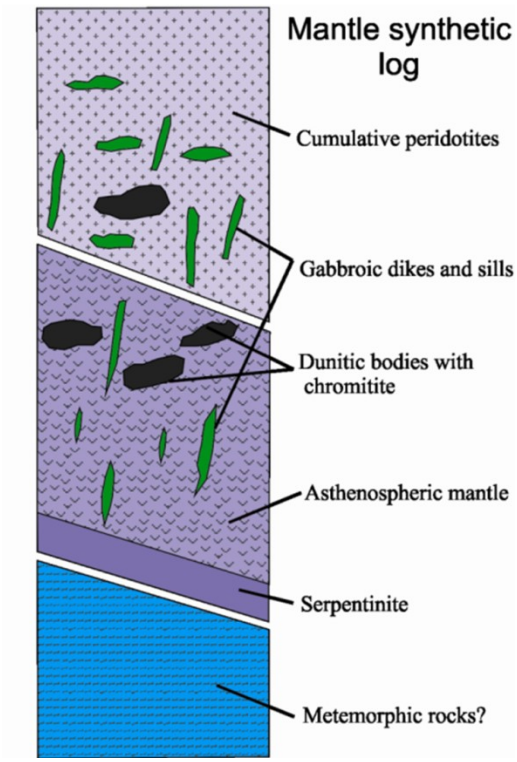

Fig 4. Schematic stratigraphic column showing the main units of the south Jazmourian mantle sequence.

Crustal sequence rocks comprise a complete sequence of the plutonic, sub-volcanic and extrusive rocks. Plutonic rocks comprises layered gabbro with variety of olivine gabbro, troctolite, pyroxene gabbro and massive gabbro (Isotropic gabbro) that have been cut by wherlitic intrusions. Pegmatitic gabbro and plagiogranite are late phases which have cut crustal plutonic and sub-volcanic sequences. The sub-volcanic rocks comprises diabasic sheeted dikes complex which covered a wide range between Maskutan and Fannuj. Dikes and alteration zones have been exposed in anywhere of these range and are contain economically minerals such as sulfides. The diabasic sheeted dikes complex are covered with a gradual contact by extrusive sequences of pillow lavas. South Jazmourian ophiolitic area is one of the ophiolitic area in Iran that have a gratual contact between diadasic sheeted dikes and pillow lavas. The extrusive sequence, comprise of alternative pillow lava, sheet flow, interbeded pelagic limestone, chert and radiolarite which in somewhere have been cut by isolated diabasic dikes. These sequence in south Maskutan village covered by paleocene flysches with angular unconformity.

3. Petrography

The peridotite samples of study area have been serpentinized in variable rate and are mainly contains lherzolite and lesser Cpx-harzburgite with porphyroclastic texture. In these rocks are seen two generations of pyroxene including primary deformed and secondry neoblast pyroxenes. The first generation of pyroxenes are porphyroclast, deformed with high-temperature plastic deformations (Undulose extinction) (Fig. 5a). But the second generation are neoblast, without plastic deformation and their crystal size is smaller than first generation and they are seen as different types in thin sections, such as exsolution, filled embayment, symplectite , inclusion, etc. The lherzolites are divided in two groups. The first group lherzolite containing porphyroclastic olivine, clinopyroxene and orthopyroxene with chrome spinel and accessory amphibole. The olivines sometimes show kink-band. Also in some cases clinopyroxene, orthopyroxene and spinel show Symplectite texture (Fig. 5b). Symplectit texture formed as reaction below:

Olivine+Garnet→Clinopyroxene+Orthopyroxene+Spinel

(Morishita and Arai 2003; Shimizu et al. 2008)

The two pyroxene generations in Cpx-harzburgite are seen also in this group of lherzolites. According to the mineral chemistry data, the first generation of pyroxene are mantle residue with chemical composition similar to abyssal peridotites but second generation pyroxenes formed in the later stage. Also, melt/peridotite interactions have caused the formation of clinopyroxene crystals within porphyroclastic orthopyroxenes (Fig. 5c). The second group of lherzolites are fine-grained, which consist of fine-grained hydrous silicate minerals

such as amphiboles (Fig. 5d). Chromitites, which often are seen as some scattered lenses within peridotite, have been affected by hydrothermal alteration processes, uvarovite-grossular, andradite and chlorite minerals formed as irregular veins within chromitites (Fig. 6). This hydrothermal alteration processes and mineral formation caused as reaction below:

Aluminian chromite+ferroan antigorite → ferrian chromite+chromian clinochlore

(Proenza et al. 1999)

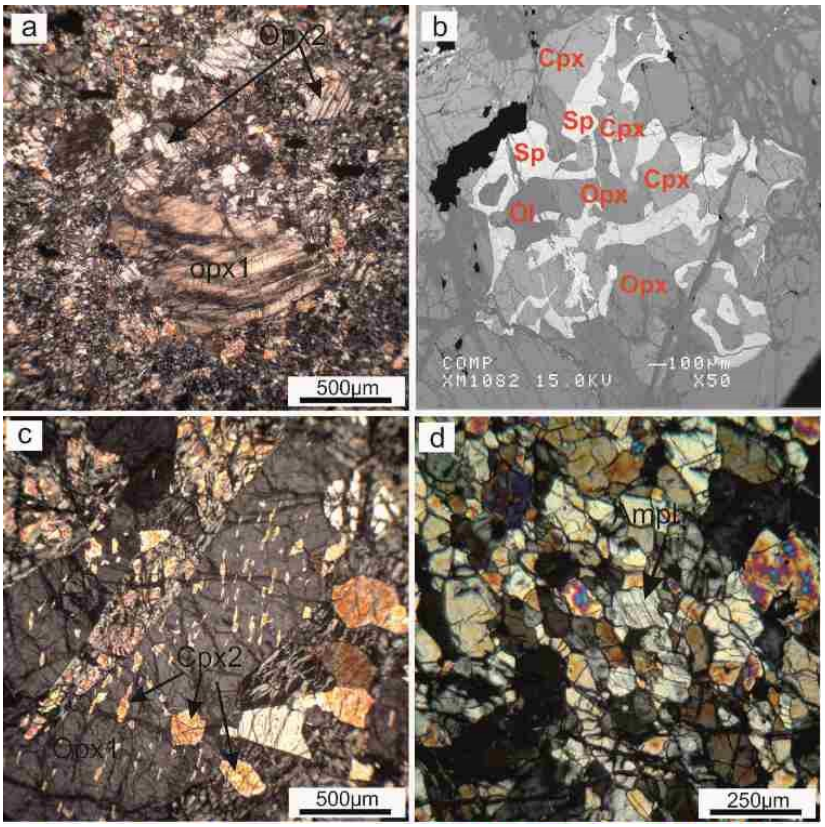

Fig 5. Photomicrographs showing textures in south Jazmourian peridotites. (a) Primary deformed orthopyroxene with undolatory extinction accompanied by neoblast orthopyroxens (south Apareng). (b) Back-Scattered electron image of spinel-pyroxene-olivine symplectite-like intergrowth (south Apareng). (c) Orthopyroxene porphyroclast with exsolution lamellae partly replaced by olivine (Ol), It also contains clinopyroxene (Cpx) inclusions (north Fannuj). (d) secondary termolitic amphiboles in fine-grained lherzolite (south Apareng).

4. Analytical methods

60 samples were collected from south Jazmourian mantle rocks. Polished thin sections were prepared for all of these samples for petrographic examination. On the basis of petrographic observations, eight samples with minimal effects of serpentinization were analyzed for major and some trace elements (Ba, Sr, Y, Zr and Zn) on inductively coupled plasma atomic emission spectrometer (ICP-AES) and other trace elements (including rare-earth elements, REE) by inductively coupled plasma mass spectrometry (ICP-MS) at SGS Laboratories of Toronto (Ontario, Canada). ICP-AES analysis used approximately 0.1 g rock powder that was first mixed with 0.9 g lithium borate in a carbon crucible and then melted in a furnace at 1100 ºC for 30 min. The fused glass samples were dissolved (using a magnetic stirring device) in 100 ml of 1% HNO_3 solution with Ge as an internal standard. ICP-MS analysis of trace elements used 0.1 g rock powders that were dissolved in a mixture of HF, HCl and HNO_3 in screw-top teflon vials. An internal standard solution containing indium was then added and the spiked sample dissolution was diluted with 1% HNO_3. The internal standard was used for monitoring drift in mass response during measurements. Representative major elements compositions of south Jazmourian peridotites are shown in Table 1.

Major-element compositions of minerals were analyzed using an electron probe micro-analyzer (JEOL JXA-8800 Superprobe) at Kanazawa University. The analyses were performed under an accelerating voltage of 15 kV and beam current of 20 nA, using a 3 µmdiameter beam. Natural and synthetic mineral standards were employed for all minerals. JEOL software using ZAF corrections was employed. Details of EPMA were described in (Morishita et al. 2003).

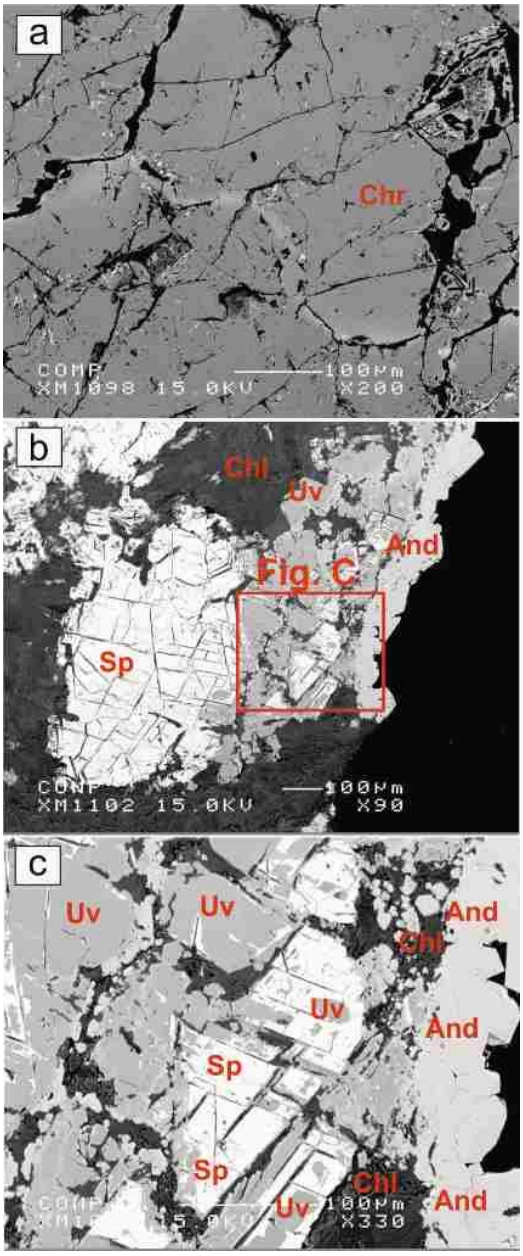

Fig 6. Back-Scattered electron image of Chromitites, affected by hydrothermal alteration, uvarovite (Uv)-grossular, andradite (And) and chlorite (Chl) minerals formed as irregular veins within chromitites.

5. Whole rock chemistry

Variable degrees of serpentinization based on different LOI contents are observed throughout the rock units. The LOI values range from 3 to 12 wt% for south Jazmourian peridotites (Table. 1).

Major elements of peridotite have been used to estimate the degree of mantle melting in different tectonic settings such as mid-ocean ridges and subduction zones (Barth et al. 2008; Niu 2004; Takazawa et al. 2000; Takazawa et al. 2003). In Fig. 7 we compare south Jazmourian peridotites with the model of near-fractional mantle melting of major elements calculated by Niu (1997) with a PM source and a pressure range of 2.5–0.4 GPa. The composition of global abyssal peridotites (Niu 2004) and SSZ peridotites (Parkinson and Pearce 1998) are shown for comparison. Despite the loss of MgO, the correlations between the oxides and the degree of mantle melting are well preserved. The content of Al_2O_3 (1.1–5.99%) corresponds to a model melting range of 13–17% (Fig 7a). The CaO of south Jazmourian peridotites decreases from 1.64% to 0.84%, corresponding to a model melting range of 16–20% (Fig. 7b). The degree of mantle melting in the model ranges from 12% to 16% when SiO_2 (37.5–41.8%) and FeO_{tot} (7.66-8.37%) is considered (Figs. 7c, 7d). CaO and Al_2O_3 are the major constituents of the mantle mineral phases and have a constant rate of decrease before the cpx is melted out (F > 25%); therefore, they can be used as a more effective means of estimating the degree of melting. Finally, if the alteration effect is corrected, a rough degree of mantle melting can be estimated for comparison with other melting indicators although they cannot represent the exact melting degree. As it is known in fig. 7, south Jazmourian peridoties lies in range between abyssal and SSZ peridoties with 10 to 20% degree of mantle melting.

6. Mineral chemistry

6.1.Olivine

Olivine compositions from south Jazmourian peridotites are shown in Fig. 8. The average forsterite (Fo) and NiO contents of olivine increase from fine-grained lherzolite (0.90 & 0.37 wt. %) to Cpx-harzburgite (0.91 & 0.38 wt. %) and to porphyroclastic lherzolites from lower part of mantle sequence (0.91 & 0.40 wt. %), respectively. The data show that average values of Fo and NiO in olivines is approximately similar in all mantle sequence and are comparable with the amounts of olivines in forearc peridotites (Ishii et al. 1992) and abyssal peridotites.'

6.2. Orthopyroxene

Orthopyroxene compositions from south Jazmourian peridotites are shown in Fig. 9. The average Mg# (= 100 Mg/(Mg+Fe) atomic ratio) of orthopyroxene is in Cpx-harzburgite 90.7 and in lherzolites 91 (Fig. 9a) that these values are considered as high Mg# values. The Al_2O_3 content of orthopyroxene usually decreases from core to rim in both types of peridotite. The Al_2O_3 contents of the cores of orthopyroxene porphyroclasts decrease from lherzolite (3.3 wt. %) to Cpx-harzburgite (3 wt. %) (Fig. 10a). The TiO_2 content same as Al_2O_3 content decreases from core to rim of orthopyroxene porphyroclasts. The average content of this oxide is in orthopyroxene cores 0.3 wt. % and in rim 0.1 wt. %.

Table 1. Major element analyses of peridotites from south Jazmourian.

Samples	FN-1	FN-2	FN-3	FN-4	FN-31	FN-114	FN-115	FN-107
Rock type				lz				cpx-hz
SiO_2 (wt%)	42.3	42.5	39.9	41.8	37.5	40.5	41.4	38
Al_2O_3	1.45	1.42	1.2	1.51	1.32	1.55	1.82	5.99
CaO	1.58	1.75	1.33	1.49	1.5	1.12	1.64	0.84
Cr_2O_3	0.4	0.42	0.52	0.41	0.33	0.4	0.42	0.4
Fe_2O_3	8.76	8.74	8.37	7.86	7.66	7.85	8.1	7.73
K_2O	0.01	0.01	0.01	0.03	0.01	0.02	0.02	0.01
MgO	44.52	44.83	41.67	40.48	38.03	40.25	40.24	39.45
MnO	0.13	0.12	0.12	0.12	0.11	0.31	0.13	0.18
Na_2O	0.1	0.1	0.1	0.1	0.1	0.1	0.2	0.1
P_2O_5	0.01	0.01	0.01	0.01	0.01	0.01	0.01	0.01
TiO_2	0.02	0.02	0.01	0.04	0.03	0.02	0.04	0.02
LOI	4.12	3.38	9.66	7.55	11.2	9.57	7.08	9.17
Sum	103.4	103.3	102.9	101.4	97.8	101.7	101.1	101.9

Abbreviations, lh: lherzolite; cpx-hz: clinopyroxene-bearing harzburgite. Normalizing values for REE ratios are from Sun and McDonough (1989).

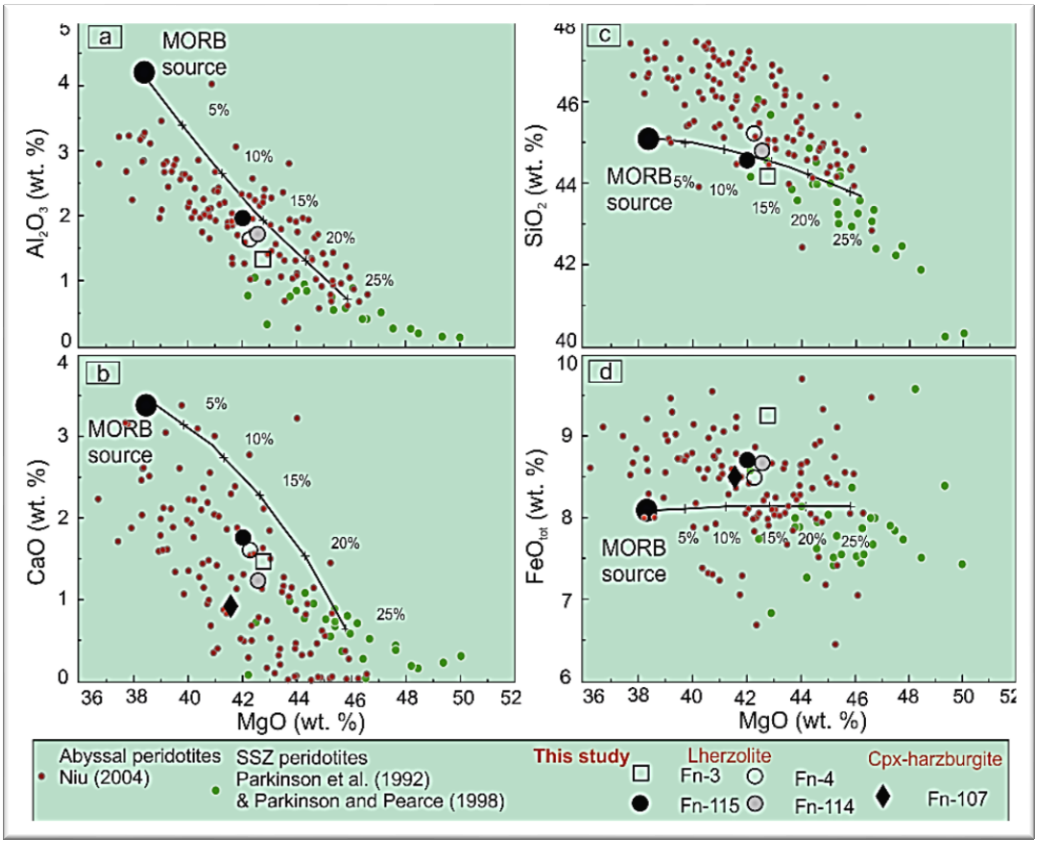

Fig 7. Plots of whole-rock MgO contents against Al_2O_3 (a), CaO (b), SiO_2 (c) and FeOtot (d) (all in wt.%). Element concentrations have been recalculated to 100% on an LOI-free basis. The calculated melting trend for residual spinel peridotites using the model of Niu (1997) is shown, which assumes anhydrous polybaric near-fractional melting of a PM source from 2.5 GPa to 0.4 GPa. Numbers along the line indicate percentage melting.

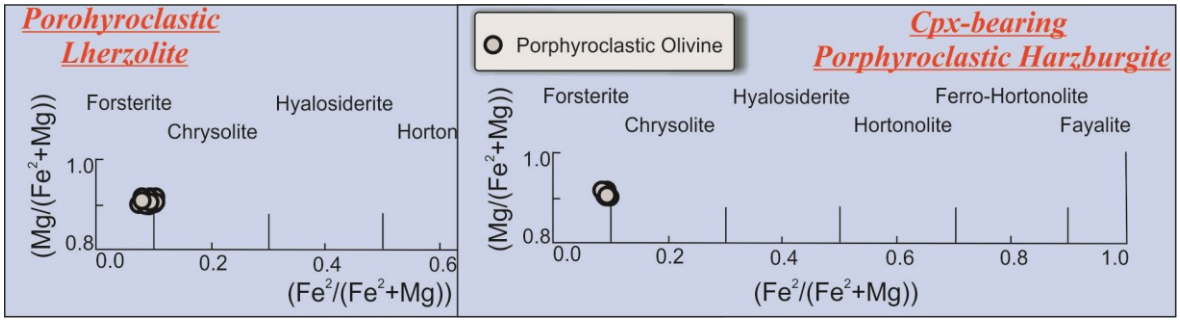

Fig 8. olivine compositions from south Jazmourian peridotites

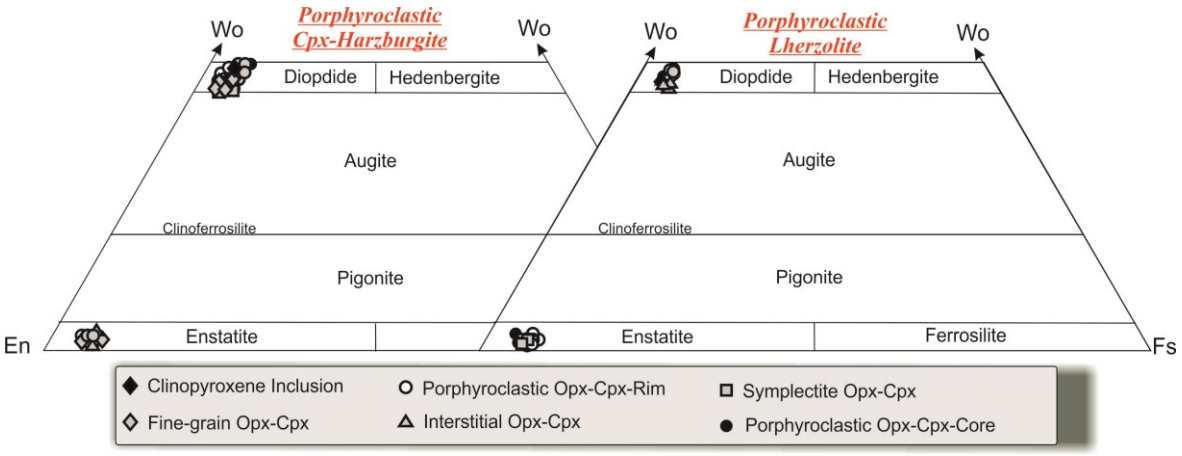

Fig 9. Orthopyroxene and Clinopyroxene compositions from south Jazmourian peridotites (Morimoto 1989).

6.3. Clinopyroxene

Clinopyroxene compositions from south Jazmourian peridotites are shown in Fig. 9. The Mg# of clinopyroxene is changing from 93 to 96, which is the highest value to fine-grained lherzolite (Fig. 10b). The Mg# of clinopyroxene porphyroclasts increase from core to rim in both types of peridotite. The Cr number (Cr #) also varies in clinopyroxene and has a different behavior with Mg#. The average Cr# of clinopyroxene is 11 in fine-grained lherzolite, about 24 in Cpx-harzburgite and 27 in porphyroclastic lherzolite (Fig. 10b). The Cr# decrease from core to rim of clinopyroxene porphyroclasts (reverse to Mg#). The maximum Cr# is related to core of porphyroclasts and the lowest is related to fine-grained neoblasts and interstitial clinopyroxenes. The average Al_2O_3 content is less than 1 wt. % in clinopyroxene of fine-grained lherzolite, about 1.5 wt. % in Cpx-harzburgite and about 3 wt. % in porphyroclastic lherzolite. The content of this oxide show decrease from core to rim of clinopyroxene in all mantle peridotites. The symplectite and exsolution clinopyroxene intergrowths with orthopyroxenes have more than 3 wt. % Al_2O_3. The lowest content of this oxide is related to fine grain clinopyroxenes and therefore, there is a positive relationship between crystal size and increase of Al_2O_3 content in clinopyroxene. The TiO_2 and Na_2O content of clinopyroxene porphyroclasts generally decreases from core to rim. The content of TiO_2 is less than 0.3 wt. % (Fig. 10c) and the content of Na_2O is less than 0.7 wt. %. The highest content of these oxides are related to clinopyroxenes that are seen as simplectite with orthopyroxene and spinel. The Cr_2O_3, Al_2O_3 and Na_2O contents in clinopyroxene from south jazmourian peridotites show decreases from porphyroclast to neoblast (fine) and core to rim (Fig. 11).

6.4. Amphibole

Amphibole compositions from south Jazmourian peridotites are shown in Fig. 12. Amphiboles in south Jazmourian peridotites occure as two types: 1) as lamellas at the rims of fresh orthopyroxene or as patches in alignment with the clinopyroxene exsolution lamellae within orthopyroxene which has a magnesiohastingsite composition (Fig. 13). 2) as fine-grained neoblast which commonly associated with altered minerals such as serpentine and talc, if formed during seawater alteration, generally has a termolitic composition.

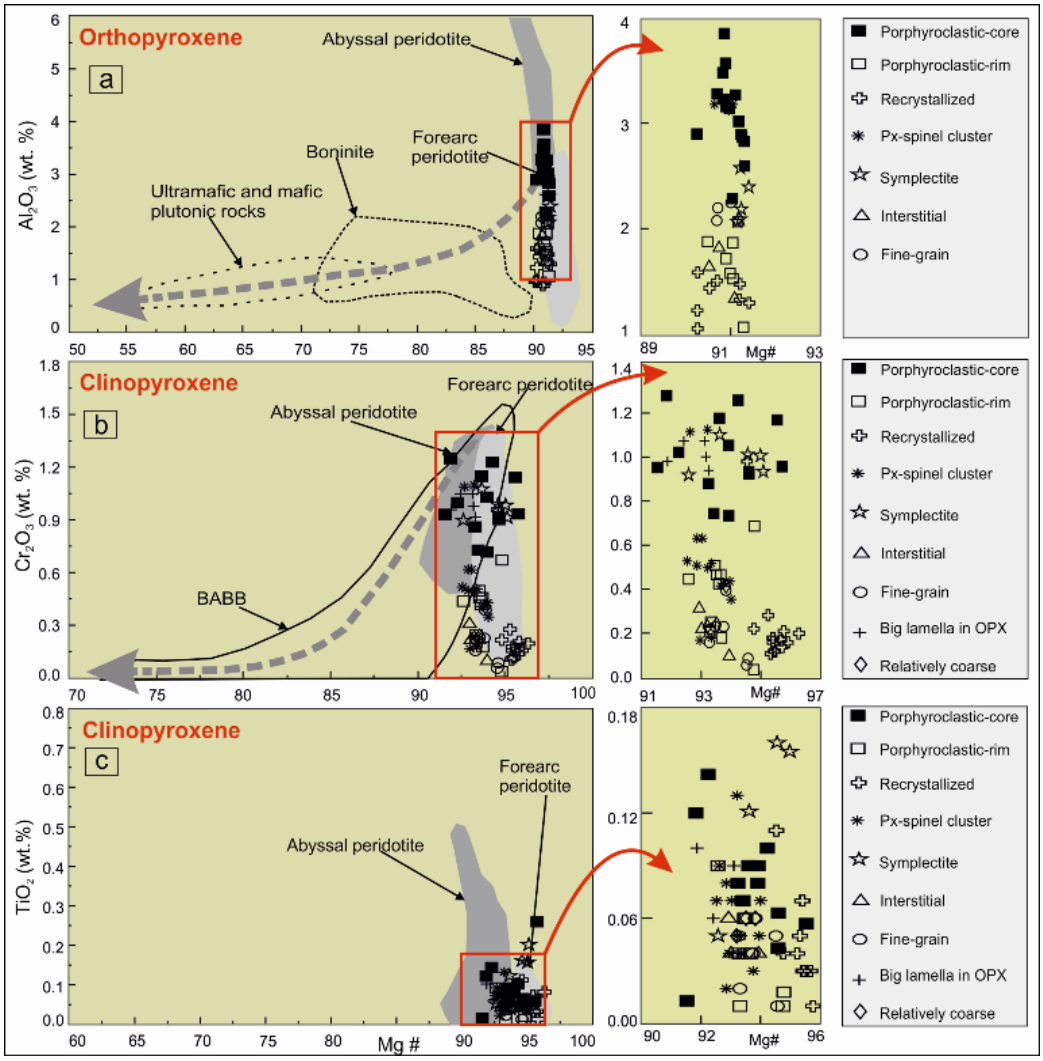

Fig 10. Composition of orthopyroxenes. (a) Al_2O_3 (wt. %) vs. Mg# of orthopyroxenes (b) Cr_2O_3 (wt. %) vs. Mg# in clinopyroxene and (c) TiO_2 (wt. %) vs. Mg# of clinopyroxenes from FMO peridotites. Abyssal peridotite field taken from (Johnson et al. 1990), forearc peridotites (Ishii et al. 1992), boninites (van der Laan et al. 1992), ultramafic and mafic plutonic rocks from Pito, Terevaka and Garrett (Constantin 1999), and Back-arc-basin basalt (BABB) field from Hawkins and Allan (1994).

Amphiboles in the fine-grained lherzolite are tremolitic and magnesio-hornblende by classification of Leake et al. (1997). Amphibole lamellae within orthopyroxene in Cpx-harzburgites are magnesio-hastingsite and amphibole in porphyroclastic lherzolite are magnesio-hornblende.

6.5. Spinel

Spinel compositions from south Jazmourian peridotites are shown in Fig. 14. Cr# [= Cr/(Cr+Al) atomic ratio] in spinel of south Jazmourian peridotites has changed from 17 to 46. But the amount of Cr# increased in spinel of some chromitite (47 to 65) (Fig. 15). The peridotites in studied area are almost homogeneous in terms of Cr# content and are similar to abyssal peridotites. Whereas, Cr# of chromitite spinels and some spinel from fine-grained lherzolite is close to values of SSZ peridotite. The amount fo TiO_2 is low in spinels of peridotite (less than 0.1 wt. %) whereas this value is reached to 0.22 wt. % in chromitites.

7. Discussion

The variability of petrographic, mineralogical and geochemical features of the peridotites from south Jazmourian suggests that they underwent a complex, multistage evolution. As mentioned before, the main mineral chemistry of south Jazmourian peridotite is a reflection of their different characteristics and petrogenesis. These various compositions, is variable from abyssal to suprasubduction zone peridotites and could be comparable with those back arc basins (Mehdipour Ghazi et al. 2010; Ohara et al. 2002). Therefore, in this part, we discuss petrogenesis of south Jazmourian mantle rocks using chemical composition of minerals and whole rock.

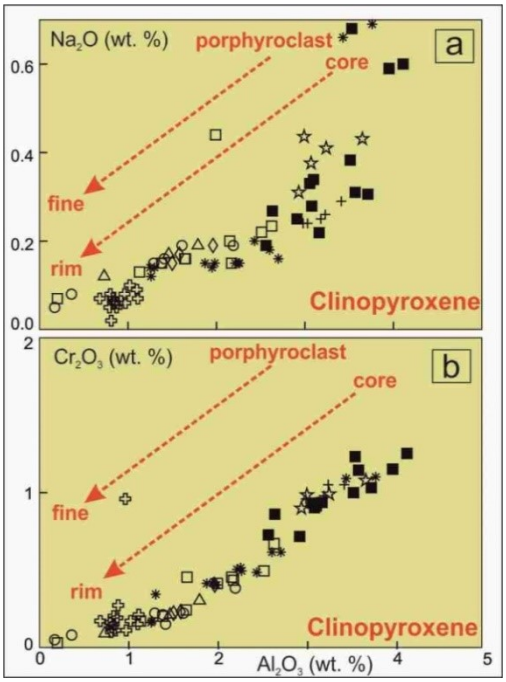

Fig 11. The Na_2O (a), Cr_2O_3 (b) and Al_2O_3 content of clinopyroxene generally decreases from porphyroclast to neoblast (fine) and core to rim. Symbols are the same as in Fig. 10.

7.1. Origin of medium-Cr# Chromitites

Based on the Cr# (=Cr/(Cr+Al) atomic ratio) of spinel, two distinctive groups, (1) low Cr# (<0.4) rocks (mainly peridotites) and (2) medium Cr# (0.4-0.65) rock (mainly chromitite), occur close to each other and chromitite associated with mildly refractory Cpx-harzburgite. Although podiform chromitites are common in subduction-related mantle settings, as represented in most, if not all, ophiolites, their occurrence in other tectonic settings is still subject to debate (Ahmed and Arai 2002; Ahmed et al. 2001; Arai and Yurimoto 1994; Morishita et al. 2007; Nicolas 2012; Zhou et al. 1998). However, there is a general consensus that high-Cr chromitites (Cr#>c. 0.60) crystallize from ultramafic boninite magmas, whereas high-Al chromitites (Cr#<c. 0.60) crystallize from less refractory MORB-like tholeiite (Arai and Yurimoto 1994; Morishita et al. 2007; Uysal et al. 2005; Zhou et al. 2001). The high-Cr podiform chromitites are thought to have formed by interaction of boninite with variably refractory peridotite (Zhou et al. 1998).

Morishita et al. (2011a) and Morishita et al. (2011b) reported that high-Cr# spinel-bearing dunite and medium-Cr# spinel-bearing dunite occur in refractory harzburgite of the Eastern Mirdita Ophiolite (EMO) Albania, and in the Izu-Bonin-Mariana (IBM) arc, respectively. Morishita et al. (2011a) suggested that the Medium-Cr# spinel-bearing dunite was caused by interaction with a melt transitional between MORB-like and boninitic melts, probably due to an increasing contribution of slab-derived fluids in an island arc setting. Morishita et al. (2011b) suggested that the Medium-Cr# dunite was a melt conduit for a FABs from the Mariana forearc that was erupted at the inception of subduction. The wide range of variation in the Cr# of spinel in south Jazmourian peridotites (Fig. 15) was probably caused by changing melt compositions in a subduction-related basin (Morishita et al. 2011a; Morishita et al. 2011b).

7.2. Origin of fine-grained lherzolites

Two types of main textures have been recognized in south Jazmourian peridotites: (1) coarse-grained porphyroclastic texture and (2) fine-grained foliated textures. The transition from porphyroclastic to fine-grained is well defined in some thin sections. The microstructures of the coarse-grained peridotites are characterized by the presence of coarse (1–3 mm) olivine, orthopyroxene and lesser clinopyroxene porphyroclasts, poorly recrystallized into small (0.1–0.3 mm) neoblasts. The olivine porphyroclasts have irregular and curved boundaries, in contrast to the smaller grains, which have more regular to polygonal boundaries. Orthopyroxene and clinopyroxene porphyroclasts, showing deformation by kinking and bending (Fig. 5a).

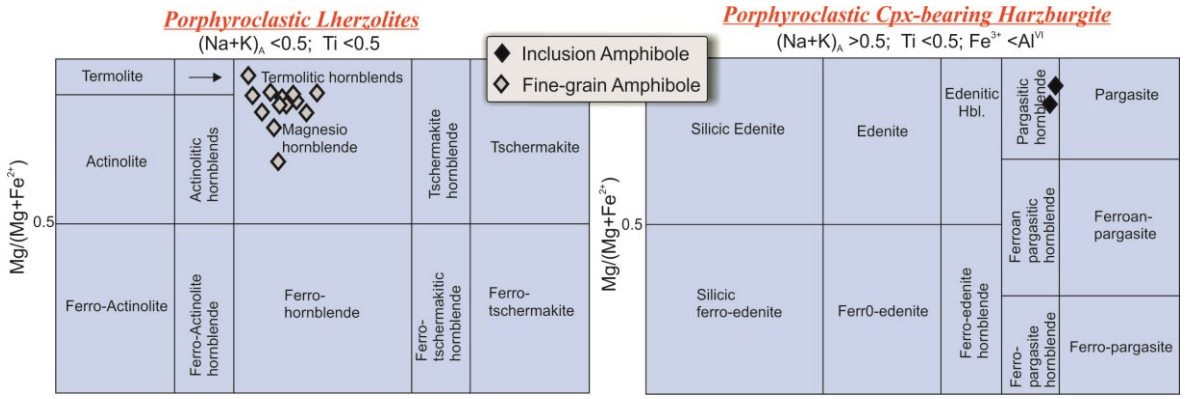

Fig 12. Amphibole compositions from south Jazmourian peridotites (Leake et al. 1997).

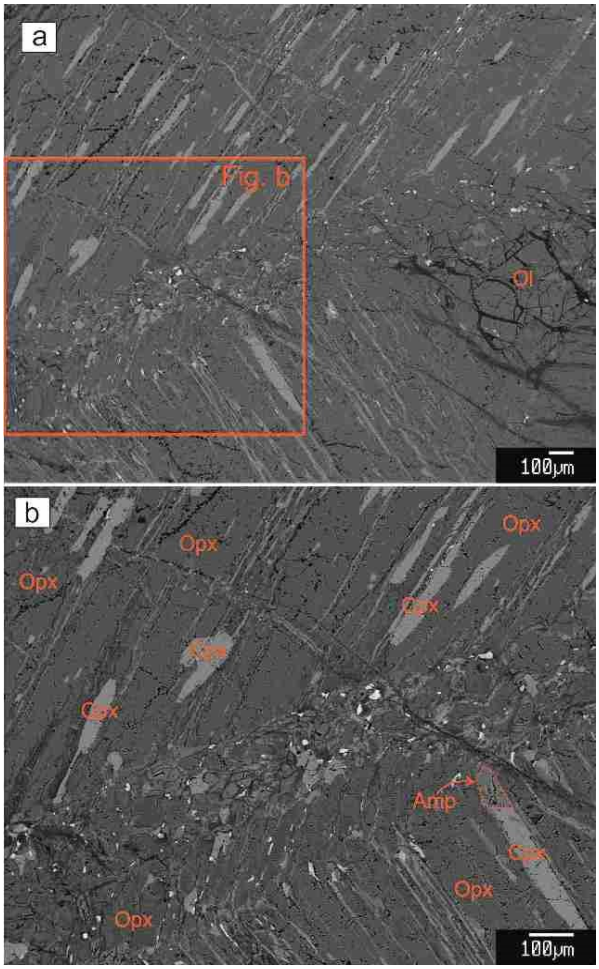

Fig 13. Back-Scattered electron image of amphibole patches in alignment with the clinopyroxene exsolution lamellae within orthopyroxene which has a magnesiohastingsite composition.

These porphyroclasts occur as isolated crystals and are oriented parallel to the main foliation and have gently curved grain boundaries embedded in the olivine matrix. These textures are considered to have formed by high-temperature deformation (1200– 1250 ºC) at solidus or hyper-solidus temperatures, related to the asthenospheric flows beneath a spreading center (Michibayashi and Mainprice 2004).

F-type peridotites are similar in their modal mineralogy to C-type peridotites; foliation occurs in some samples. Olivine is around 60-70 µm across and contains minute inclusions of chromian spinel and bubbles (Schiano et al. 1995). The proposal of two possibilities for the origin of fine-grained peridotite (F-type) could be: (i) metasomatic origin from coarse-grain peridotite (C-type) and (ii) deserpentinization origin from some abyssal serpentinite of which protolith was the C-type peridotite (Arai et al. 1996). Arai and Kida (2000) concluded that the fine-grained peridotites were formed by fluid metasomatism, or alternatively, but less possibly, by deserpentinization of serpentinite in the mantle wedge. Also, Arai et al. (2004) proposed that the formation of F-type peridotites from C-type peridotites was due to shearing of the mantle wedge by oblique subduction. This may be common within supra-subduction zone mantle wedges because oblique subduction is common. Another authors proposed that these fabrics are result of deformation, linked to the lithospheric flows at lower temperature (1000–1100ºC) and higher stress conditions (Michibayashi and Mainprice 2004; Monsef et al. 2010).

7.3. mantle metasomatism or Melt/rock interaction

Also, south Jazmourian peridotites provide abundant field and textural evidence for an important role of melt percolation and melt/rock reactions relatively late in their history. In the field, millimeter- to centimeter-scale gabbroic veins are widespread (Figs. 4c, d). These features suggest that melts traversed the peridotites in a localized way (Dijkstra et al. 2009). Textural evidence for pervasive porous melt flow and concomitant melt/rock reactions causing modal metasomatism can be found in some samples. Texture is strikingly similar to those in peridotites from Ocean Drilling Program (ODP) hole 1274A at the fifteen twenty fracture zone (Suhr et al. 2008) and those from Macquarie Island (Dijkstra et al. 2009). Orthopyroxene clasts have a corroded, holly leaf-like or skeletal appearance, containing numerous embayments of olivine (Figs. 16a, b). Such textures are generally considered to be evidence for porous flow of orthopyroxene-under saturated melts, which dissolve orthopyroxene by a melt-producing melt/rock reaction (Dijkstra et al. 2003; Dijkstra et al. 2009; Kelemen et al. 1992; Piccardo et al. 2007; Suhr et al. 2008).

7.4. Geotectonic setting

SSZ peridotites are characterized by spinels with much higher Cr#s than abyssal peridotites, ranging from around 38 to over 80, which indicates significantly higher degrees of partial melting in the SSZ peridotites compared to abyssal peridotites (Arai 1994; Gaetani and Grove 1998). There is significant overlap with spinel from abyssal peridotites from Cr#s 38 to 58 (Fig. 15) and a significant number of spinel of south Jazmourian peridotites are placed in this area. Spinel Cr # values in the spinel of studied area is a wide range from 17 to 67, which covers together abyssal and a part of SSZ peridotites. These values have full overlap with the Cr# values of spinel from back-arc basin peridotites (Monnier et al. 1995).

It has been demonstrated that both supra-subduction and abyssal peridotites can be juxtaposed in the same ophiolite, reflecting the fact that an ophiolite can experience a multi-stage evolution in different tectonic settings (Batanova and Sobolev 2000; Choi et al. 2008).

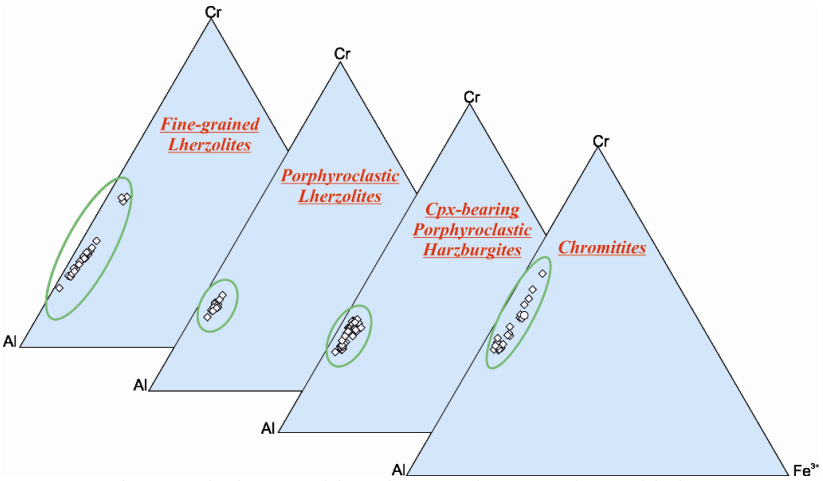

Fig 14. Spinel compositions from south Jazmourian peridotites.

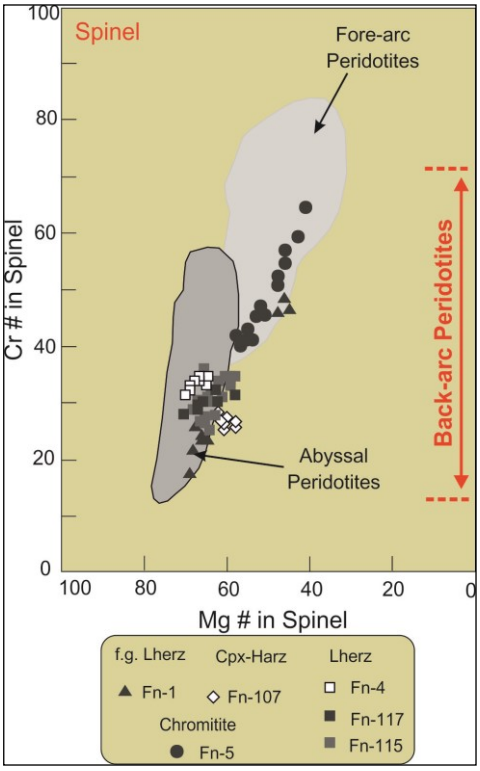

Fig 15. Cr# versus Mg# in the studied spinels. Field of fore-arc and abyssal peridotites from Tamura and Arai (2006), back arc peridotites from Monnier et al. (1995).

The reaction of south Jazmourian peridotites with hydrous melts of subduction affinity provides compelling support that they underwent modification in a subduction zone setting. Juxtaposition of both abyssal and SSZ peridotites suggests that south Jazmourian ophiolite has experienced a multi-stage evolution. First, the mantle peridotites were depleted by melt extraction, probably beneath a medium to fast-spreading ridge, during which the initial precursor of south Jazmourian ophiolite formed. Subsequently, these abyssal-type peridotites entered an intraoceanic subduction zone during the closure of the Neo-Tethys Ocean. There they were metasomatized by arc magmas derived from the mantle wedge, resulting in the formation of medium-Cr# chromitite and enrichment LREE in peridotites. Therefore, we suggest that mantle peridotites outcropping along south Jazmourian record both the opening of the Neo-Tethys Ocean and its closure through subduction.

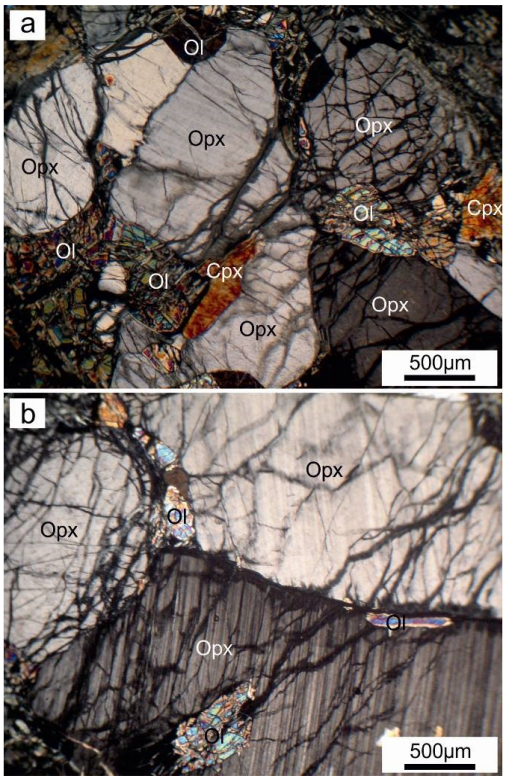

Fig 16. Photomicrographs (crossed polarizers) showing evidence for melt-peridotite reactions in south Jazmourian peridotites. (a,b) Corroded orthopyroxenes (opx), corrosion embayments filled by olivine (ol), sample Fn-31.

7. Conclusion

A large set of internally consistent analytical data, including primary mineralogy and bulk rock chemistry are first presented for mantle sequence rocks from south Jazmourian. A range of mineralogical, geochemical and petrological criteria for recognition of the probable geodynamic setting of the origin of peridotite and chromitite is proposed, discussed and applied to mantle sequence of south Jazmourian.

Mantle sequence of south Jazmourian comprise clinopyroxene bearing harzburgite, lherzolite, fine-grained lherzolite, rodingitized gabbroic dikes and chromitite lenses which are seen as scattered within mantle sequence. These units have preserved textural evidences related to the mantle and asthenosphere, although they have been strongly serpentinized the range of spinel Cr# in south Jazmourian peridotites is very wide (0.17–0.45), and it is even broader if chromite segregations (0.35–0.65) are taken into account. This is not consistent with formation of south Jazmourian peridotites in slow-spreading, fast-spreading, or anomalous MORB settings. This rang covers together abyssal and a part of SSZ peridotites. These values have full overlap with the Cr# values of spinel from back-arc basin peridotites.

Although, south Jazmourian peridotites display petrographic, mineralogical, and geochemical characteristics, which are both abyssal and SSZ type ophiolites. REE modelling shows that depleted lherzolite have REE compositions similar to those of residual MORB mantle rocks, which experienced 5–15% removal of MORB melts. But, the significant LREE/ MREE enrichment observed in all peridotites suggests these rocks represent residual MORB mantle enriched in LREE by fluids released from the subducting slab in a SSZ setting. Therefore, we propose that south Jazmourian has experienced a multi-stage evolution, the first stage was formation at a mid-ocean ridge and the second was the subsequent transfer to a subduction zone setting. These rocks thus record both the opening and subsequent closure of the Neo-Tethys Ocean.

Acknowledgements

This work is an output of research project (14-11-5-10996) which supported by Islamic Azad University of Zahedan Branch. Financial support through this project from Islamic Azad University of Zahedan Branch acknowledged.

References

Ahmed A, Arai S (2002) Unexpectedly high-PGE chromitite from the deeper mantle section of the northern Oman ophiolite and its tectonic implications, *Contributions to Mineralogy and Petrology* 143:263-278.

Ahmed AH, Arai S, Attia AK (2001) Petrological characteristics of podiform chromitites and associated peridotites of the Pan African Proterozoic ophiolite complexes of Egypt, *Mineralium Deposita* 36:72-84.

Arai S (1994) Compositional variation of olivine-chromian spinel in Mg-rich magmas as a guide to their residual spinel peridotites, *Journal of Volcanology and Geothermal Research* 59:279-293.

Arai S, Kida M (2000) Origin of fine-grained peridotite xenoliths from Iraya volcano of Batan Island, Philippines: deserpentinization or metasomatism at the wedge mantle beneath an incipient arc?, *Island Arc* 9:458-471.

Arai S, Kida M, Abe N, Ninomiya A (1996) Classification of peridotite xenoliths in cale-alkaline andesite from Iraya volcano, Batan Island, the Philippines, and its genetical implications, *The science reports of the Kanazawa University* 41:25-45.

Arai S, Takada S, Michibayashi K, Kida M (2004) Petrology of peridotite xenoliths from Iraya volcano, Philippines, and its implication for dynamic mantle-wedge processes, *Journal of Petrology* 45:369-389.

Arai S, Yurimoto H (1994) Podiform chromitites of the Tari-Misaka ultramafic complex, southwestern Japan, as mantle-melt interaction products, *Economic Geology* 89:1279-1288.

Barth MG, Mason PR, Davies GR, Drury MR (2008) The Othris Ophiolite, Greece: a snapshot of subduction initiation at a mid-ocean ridge, *Lithos* 100:234-254.

Batanova VG, Sobolev AV (2000) Compositional heterogeneity in subduction-related mantle peridotites, Troodos massif, Cyprus, *Geology* 28:55-58.

Choi SH, Shervais JW, Mukasa SB (2008) Supra-subduction and abyssal mantle peridotites of the Coast Range ophiolite, California, *Contributions to Mineralogy and Petrology* 156:551.

Constantin M (1999) Gabbroic intrusions and magmatic metasomatism in harzburgites from the Garrett transform fault: implications for the nature of the mantle–crust transition at fast-spreading ridges, *Contributions to Mineralogy and Petrology* 136:111-130.

Desmons J, Beccaluva L (1983) Mid-ocean ridge and island-arc affinities in ophiolites from Iran: palaeographic implications: complementary reference, *Chemical Geology* 39:39-63.

Dijkstra AH, Barth MG, Drury MR, Mason PR, Vissers RL (2003) Diffuse porous melt flow and melt-rock reaction in the mantle lithosphere at a slow-spreading ridge: A structural petrology and LA-ICP-MS study of the Othris Peridotite Massif (Greece), *Geochemistry, Geophysics, Geosystems* 4.

Dijkstra AH, Sergeev DS, Spandler C, Pettke T, Meisel T, Cawood PA (2009) Highly refractory peridotites

on Macquarie Island and the case for anciently depleted domains in the Earth's mantle, *Journal of Petrology* 51:469-493.

Farhoudi G, Karig D (1977) Makran of Iran and Pakistan as an active arc system, *Geology* 5:664-668.

Gaetani GA, Grove TL (1998) The influence of water on melting of mantle peridotite, *Contributions to Mineralogy and Petrology* 131:323-346.

Ghazi AM, Hassanipak AA, Mahoney JJ, Duncan RA (2004) Geochemical characteristics, 40Ar–39Ar ages and original tectonic setting of the Band-e-Zeyarat/Dar Anar ophiolite, Makran accretionary prism, S.E. Iran, *Tectonophysics* 393:175-196.

Glennie K, Clarke MH, Boeuf M, Pilaar W, Reinhardt B (1990) Inter-relationship of Makran-Oman Mountains belts of convergence, *Geological Society, London, Special Publications* 49:773-786.

Glennie KW (2000) Cretaceous tectonic evolution of Arabia's eastern plate margin: a tale of two oceans. In: Middle East Models of Jurassic–Cretaceous Carbonate Systems, edited by Alsharhan AS and Scott RW 69: 9-20.

Gregory RT, Gray DR, Miller JM (1998) Tectonics of the Arabian margin associated with the formation and exhumation of high-pressure rocks, Sultanate of Oman, *Tectonics* 17:657-670.

Hawkins J, Allan J Petrologic evolution of Lau Basin sites 834 through 839. In: Proceedings of the Ocean Drilling Program. Scientific Results, 1994. Ocean Drilling Program, pp 427-470.

Hunziker D, Burg J-P, Caddick M, Reusser E, Omrani J Blueschists of the Inner Makran accretionary wedge, SE Iran: Petrography, geochemistry and thermobarometry. In: EGU General Assembly Conference Abstracts, 2010. p 1572.

Ishii T, Robinson PT, Maekawa H, Fiske R (1992) Petrological studies of peridotites from diapiric serpentinite seamounts in The Izu–Ogasawara–Mariana forearc, LEG125. In: Fryer, P., Pearce, J.A., Stokking, L.B. (Eds.), Proceedings of the Ocean Drilling Program, *Ocean Drilling Program, College Station, Texas* 125:445-485.

Johnson K, Dick HJ, Shimizu N (1990) Melting in the oceanic upper mantle: an ion microprobe study of diopsides in abyssal peridotites, *Journal of Geophysical Research: Solid Earth* 95:2661-2678.

Juteau T, Maury R (2012) La croûte océanique: pétrologie et dynamique endogènes: cours & exercices corrigés: licence et master, sciences de la terre et de l'environnement. Vuibert.

Kananian A (2000) Petrology and Geochemistry of Kahnouj Ophiolitic Complex. PhD Thesis, Department of Geology, Tarbiat Modares University, Tehran, Iran. Published Thesis, (in Persion).

Kelemen PB, Dick HJ, Quick JE (1992) Formation of harzburgite by pervasive melt/rock reaction in the upper mantle, *Nature* 358:635-641.

Knipper A, Ricou L-E, Dercourt J (1986) Ophiolites as indicators of the geodynamic evolution of the Tethyan ocean, *Tectonophysics* 123:213-240.

Kopp C, Fruehn J, Flueh E, Reichert C, Kukowski N, Bialas J, Klaeschen D (2000) Structure of the Makran subduction zone from wide-angle and reflection seismic data, *Tectonophysics* 329:171-191.

Leake BE et al. (1997) Report. Nomenclature of amphiboles: report of the subcommittee on amphiboles of the international mineralogical association commission on new minerals and mineral names, *Mineralogical magazine* 61:295-321.

Marchesi C (2006) Petrogenesis of the ultramafic and mafic rocks from the Mayarí-Baracoa Ophiolitic Belt and the spatially-related volcanism (Eastern Cuba).

McCall G (1985) Area report, east Iran, area no. 1, *Geological Survey of Iran Report* 57:643.

McCall G (1997) The geotectonic history of the Makran and adjacent areas of southern Iran, *Journal of Asian Earth Sciences* 15:517-531.

McCall G (2002) A summary of the geology of the Iranian Makran, *Geological Society, London, Special Publications* 195:147-204.

McCall G (2003) A critique of the analogy between Archaean and Phanerozoic tectonics based on regional mapping of the Mesozoic-Cenozoic plate convergent zone in the Makran, Iran, *Precambrian Research* 127:5-17.

McCall G, Kidd R (1982) The Makran, Southeastern Iran: the anatomy of a convergent plate margin active from Cretaceous to Present, *Geological Society, London, Special Publications* 10:387-397.

Mehdipour Ghazi J, Moazzen M, Rahgoshay M, Moghadam S (2010) Mineral chemical composition and geodynamic significance of peridotites from Nain ophiolite, central Iran, *Journal of Geodynamics* 49:261-270.

Michibayashi K, Mainprice D (2004) The role of pre-existing mechanical anisotropy on shear zone development within oceanic mantle lithosphere: an example from the Oman ophiolite, *Journal of Petrology* 45:405-414.

Mohajeran K (1998) Petrological studies of Sarzeh ophiolitic area, Northern Fannuj, Sistan and Baluchistan province. M.Sc. Thesis, Department of Geology, Tabriz University, Tabriz, Iran. Published Thesis, (in Persion).

Monnier C, Girardeau J, Maury RC, Cotten J (1995) Back-arc basin origin for the East Sulawesi ophiolite (eastern Indonesia), *Geology* 23:851-854.

Monsef I, Rahgoshay M, Mohajjel M, Moghadam HS (2010) Peridotites from the Khoy Ophiolitic Complex, NW Iran: Evidence of mantle dynamics in a supra-subduction-zone context, *Journal of Asian Earth Sciences* 38:105-120

Morimoto N (1989) Nomenclature of pyroxenes, *Mineralogical Journal* 14:198-221.

Morishita T, Arai S (2003) Evolution of spinel-pyroxene symplectite in spinel-lherzolites from the Horoman Complex, Japan, *Contributions to Mineralogy and Petrology* 144:509-522.

Morishita T, Arai S, Tamura A (2003) Petrology of an apatite-rich layer in the Finero phlogopite–peridotite, Italian Western Alps; implications for evolution of a metasomatising agent, *Lithos* 69:37-49.

Morishita T, Dilek Y, Shallo M, Tamura A, Arai S (2011a) Insight into the uppermost mantle section of a maturing arc: the Eastern Mirdita ophiolite, Albania, *Lithos* 124:215-226.

Morishita T, Maeda J, Miyashita S, Kumagai H, Matsumoto T, Dick HJ (2007) Petrology of local concentration of chromian spinel in dunite from the slow-spreading Southwest Indian Ridge, *European Journal of Mineralogy* 19:871-882.

Morishita T, Tani K, Shukuno H, Harigane Y, Tamura A, Kumagai H, Hellebrand E (2011b) Diversity of melt conduits in the Izu-Bonin-Mariana forearc mantle: Implications for the earliest stage of arc magmatism, *Geology* 39:411-414.

Moslempour ME, Khalatbari-Jafari M, Ghaderi M, Yousefi H, Shahdadi S (2015) Petrology, geochemistry and tectonics of the extrusive sequence of Fannuj-Maskutan ophiolite, Southeastern Iran, *Journal of the Geological Society of India* 85:604-618.

Moslempour ME, Khalatbari-Jafari M, Morishita T, Ghaderi M (2013) Petrology and Geochemistry of Peridotites from Fannuj-Maskutan Ophiolitic Complex, Makran Zone, SE Iran, *Scientific Quarterly Journal, Geosciences* 87:181-196.

Nicolas A (2012) Structures of ophiolites and dynamics of oceanic lithosphere vol 4. Springer Science & Business Media.

Niu Y (1997) Mantle melting and melt extraction processes beneath ocean ridges: evidence from abyssal peridotites, *Journal of Petrology* 38:1047-1074.

Niu Y (2004) Bulk-rock major and trace element compositions of abyssal peridotites: implications for mantle melting, melt extraction and post-melting processes beneath mid-ocean ridges, *Journal of Petrology* 45:2423-2458.

Ohara Y, Stern RJ, Ishii T, Yurimoto H, Yamazaki T (2002) Peridotites from the Mariana Trough: first look at the mantle beneath an active back-arc basin, *Contributions to Mineralogy and Petrology* 143:1-18.

Omrani H, Moazzen M, Oberhänsli R, Moslempour M (2017) Iranshahr blueschist: subduction of the inner Makran oceanic crust, *Journal of Metamorphic Geology* 35:373-392.

Parkinson IJ, Pearce JA (1998) Peridotites from the Izu–Bonin–Mariana forearc (ODP Leg 125): evidence for mantle melting and melt–mantle interaction in a supra-subduction zone setting, *Journal of Petrology* 39:1577-1618.

Piccardo G, Zanetti A, Müntener O (2007) Melt/peridotite interaction in the Southern Lanzo peridotite: field, textural and geochemical evidence, *Lithos* 94:181-209.

Proenza J, Solé J, Melgarejo J (1999) Uvarovite in podiform chromitite; the Moa-Baracoa ophiolitic massif, Cuba, *The Canadian Mineralogist* 37:679-690.

Rastin M (1999) Geochemistry and Petrology of Mokhtarabad-Remshak Ophiolitic Complex, located in Makran Zone-SE Kerman, M.Sc. Thesis, Department of Geology, Kerman University, Kerman, Iran. Published Thesis, (in Persion).

Ricou L (1977) Le croissant ophiolitique pe'ri-arabe, Une ceinture de nappes mises en place au Cre'tace'supe'rieur, *Rev Géogr phys Géol dynam*:327-350.

Schiano P, Clocchiatti R, Shimizu N, Maury R, Jochum K, Hofmann A (1995) Hydrous, silica-rich melts in the sub-arc mantle and their relationship with erupted arc lavas, *Nature* 377:595-600.

Sengor AMC, Altiner D, Cin A, Ustaomer T, Hsu KJ (1998) The Tethyside orogenic collage. In: Audley-Charles, M.G., Hallam, A. (Eds.), Gondwana and Tethys, *Geological Society and Oxford University Press, Special Publication of the Geological Society* 37:119–181.

Shahabpour J (2010) Tectonic implications of the geochemical data from the Makran igneous rocks in Iran, *Island Arc* 19:676-689.

Shaker Ardakani A (2009) Morphology and petrogenesis of pillow lavas from the Ganj Ophiolitic Complex, southeastern Kerman, Iran, *Journal of Sciences, Islamic Republic of Iran* 20.

Shimizu Y, Arai S, Morishita T, Ishida Y (2008) Origin and significance of spinel–pyroxene symplectite in lherzolite xenoliths from Tallante, SE Spain, *Mineralogy and Petrology* 94:27-43.

Shojaat B, Hassanipak A, Mobasher K, Ghazi A (2003) Petrology, geochemistry and tectonics of the Sabzevar ophiolite, North Central Iran, *Journal of Asian Earth Sciences* 21:1053-1067.

Stöcklin J (1974) Possible ancient continental margins in Iran. In: The geology of continental margins. Springer, pp 873-887.

Suhr G, Kelemen P, Paulick H (2008) Microstructures in Hole 1274A peridotites, ODP Leg 209, Mid-Atlantic Ridge: Tracking the fate of melts percolating in peridotite as the lithosphere is intercepted, *Geochemistry, Geophysics, Geosystems* 9.

Sun S-S, McDonough W-s (1989) Chemical and isotopic systematics of oceanic basalts: implications for mantle composition and processes, *Geological Society, London, Special Publications* 42:313-345.

Takazawa E, Frey FA, Shimizu N, Obata M (2000) Whole rock compositional variations in an upper mantle peridotite (Horoman, Hokkaido, Japan): are they consistent with a partial melting process?, *Geochimica et Cosmochimica Acta* 64:695-716.

Takazawa E, Okayasu T, Satoh K (2003) Geochemistry and origin of the basal lherzolites from the northern Oman ophiolite (northern Fizh block), *Geochemistry, Geophysics, Geosystems* 4.

Takin M (1972) Iranian geology and continental drift in the Middle East, *Nature* 235:147-150.

Tamura A, Arai S (2006) Harzburgite–dunite–orthopyroxenite suite as a record of supra-subduction zone setting for the Oman ophiolite mantle, *Lithos* 90:43-56.

Uysal I, Sadiklar M, Tarkian M, Karsli O, Aydin F (2005) Mineralogy and composition of the chromitites and their platinum-group minerals from Ortaca (Mugla-SW Turkey): evidence for ophiolitic chromitite genesis, *Mineralogy and petrology* 83:219-242.

van der Laan SR, Arculus R, Pearce J, Murton B Petrography, mineral chemistry, and phase relations of the basement boninite series of Site 786, Izu-Bonin forearc. In: Proceedings of the ocean drilling program, scientific results, 1992. College Station: Texas, pp 171-201.

Zhou M-F et al. (2001) Melt/mantle interaction and melt evolution in the Sartohay high-Al chromite deposits of the Dalabute ophiolite (NW China), *Journal of Asian Earth Sciences* 19:517-534.

Zhou M-F, Sun M, Keays RR, Kerrich RW (1998) Controls on platinum-group elemental distributions of podiform chromitites: a case study of high-Cr and high-Al chromitites from Chinese orogenic belts, *Geochimica et Cosmochimica Acta* 62:677-688.